

# Bifunctional Poly(acrylamide) Hydrogels through Orthogonal Coupling Chemistries

Aleeza Farrukh,<sup>†,‡</sup> Julieta I. Paez,<sup>\*,†,‡,§</sup> Marcelo Salierno,<sup>‡,§,||</sup> Wenqiang Fan,<sup>§,||</sup> Benedikt Berninger,<sup>§,||</sup> and Aránzazu del Campo<sup>\*,†,‡,⊥</sup>

<sup>†</sup>INM—Leibniz Institute for New Materials, Campus D2 2, 66123 Saarbrücken. Germany

<sup>‡</sup>Max-Planck-Institut für Polymerforschung, Ackermannweg 10, 55128 Mainz, Germany

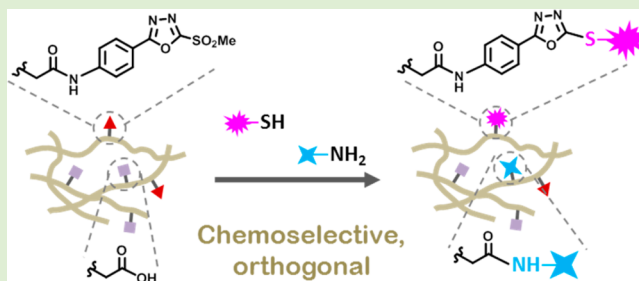
<sup>§</sup>Institute of Physiological Chemistry, University Medical Center, Johannes Gutenberg University Mainz, Hanns-Dieter-Hüsch-Weg 19, 55128 Mainz, Germany

<sup>||</sup>Focus Program Translational Neuroscience, Johannes Gutenberg University Mainz, Langenbeck strasse 1, 55131 Mainz, Germany

<sup>⊥</sup>Chemistry Department, Saarland University, 66123 Saarbrücken, Germany

## Supporting Information

**ABSTRACT:** Biomaterials for cell culture allowing simple and quantitative presentation of instructive cues enable rationalization of the interplay between cells and their surrounding microenvironment. Poly(acrylamide) (PAAm) hydrogels are popular 2D-model substrates for this purpose. However, quantitative and reproducible biofunctionalization of PAAm hydrogels with multiple ligands in a trustable, controlled, and independent fashion is not trivial. Here, we describe a method for bifunctional modification of PAAm hydrogels with thiol- and amine-containing biomolecules with controlled densities in an independent, orthogonal manner. We developed copolymer networks of AAm with 9% acrylic acid and 2% *N*-(4-(5-(methylsulfonyl)-1,3,4-oxadiazol-2-yl)phenyl)acrylamide. The covalent binding of thiol- and amine-containing chromophores at tunable concentrations was demonstrated and quantified by UV spectroscopy. The morphology, mechanical properties, and homogeneity of the copolymerized hydrogels were characterized by scanning electron microscopy, dynamic mechanical analysis, and confocal microscopy studies. Our copolymer hydrogels were bifunctionalized with polylysine and a laminin-mimetic peptide using the specific chemistries. We analyzed the effect of binding protocol of the two components in the maturation of cultured postmitotic cortical neurons. Our substrates supported neuronal attachment, proliferation, and neuronal differentiation. We found that neurons cultured on our hydrogels bifunctionalized with ligand-specific chemistries in a sequential fashion exhibited higher maturation at comparable culture times than using a simultaneous bifunctionalization strategy, displaying a higher number of neurites, branches, and dendritic filopodia. These results demonstrate the relevance of quantitative and optimized coupling chemistries for the performance of simple biomaterials and with sensitive cell types.



## 1. INTRODUCTION

Cell fate is tightly regulated *in vivo* by the coordinated presentation of biochemical cues (tethered ligands and soluble factors) and biophysical cues (like matrix elasticity) over multiple time and length scales.<sup>1,2</sup> The cooperative effect of such multiple factors is difficult to address on standard tissue culture plates, with poor control over tethered proteins and mechanical properties very different than those of the natural matrix. New materials allowing for a simple and quantitative orchestration of multiple factors are needed to progress in our understanding of the interplay between cells and their surrounding environment.<sup>3</sup>

During the past decade, researchers have recognized the potential of combining different cues on a single model platform to map and instruct cell behavior.<sup>4</sup> Poly(acrylamide) (PAAm) hydrogels have become very popular among biology

laboratories as 2D model substrates with defined biochemical and mechanical properties. These hydrogels are cost-effective, easy to prepare, reproducible, and available in a wide range of stiffness (elastic moduli  $\sim 0.1$ – $100$  kPa).<sup>5–8</sup>

Biofunctionalization of PAAm hydrogels with bioactive ligands (cell adhesive proteins or peptides, growth factors, etc.) in a controlled and functional fashion is not trivial because of the low reactivity of the amide side groups. PAAm hydrogels are frequently functionalized by physical coating of proteins on the surface, either by incubation with the protein solution or by transferring the protein from a prefucionalized glass coverslip during gel preparation.<sup>9</sup> The latter method typically leads to a

Received: December 1, 2016

Revised: January 21, 2017

Published: February 1, 2017

higher protein density on the gel surface and can be further extended to create protein micropatterns.<sup>9,10</sup> Although these methods have been successfully applied for mechanobiology studies, reproducibility and long-term stability of the coated material during the cell culture experiment is always a critical issue in physically coated PAAm. Covalent binding strategies for functionalization involve hydrogel activation with hydrazine, periodate, UV or  $\gamma$ -ray, or the use of the photoreactive bifunctional linker sulfo-SANPAH.<sup>11–13</sup> These coupling strategies involve toxic chemicals, irradiation steps, and poor selectivity for binding sites; however, they typically show low reproducibility. Copolymerization of PAAm hydrogels with reactive monomers has also been explored.<sup>6,14</sup> In this case, the resulting copolymer is expected to keep the biocompatibility and antifouling of PAAm hydrogels, to be incorporated randomly, and to not disturb PAAm polymerization kinetics and final properties. Recently, we reported methylsulfonyl-functionalized PAAm hydrogels by copolymerizing benzothiazole- and oxadiazole-derived methylsulfonyl comonomers with acrylamide (AAm). These hydrogels allowed quantitative covalent coupling of thiol-containing ligands at physiological conditions and low reaction times (minutes)<sup>15</sup> to form a stable bioconjugate. Our strategy outperformed the nonselective sulfo-SANPAH-mediated coupling<sup>8,16,17</sup> regarding functional and reproducible loading of ligands in a controlled density.

PAAm hydrogels have been used as suitable soft substrates to culture neuronal cells.<sup>18–21</sup> PAAm hydrogels of variable compliance and functionalized with adhesive factors have been applied to differentiate neurons,<sup>18</sup> as platforms for mechanosensing studies of astrocytes,<sup>22</sup> or to modulate the formation and activity of cortical neuronal networks.<sup>23</sup> In order to support attachment of neuronal cells on PAAm hydrogels, either charged ligands like poly-D-lysine (PDL)<sup>24</sup> or integrin-responsive ligands from extracellular matrix (ECM) molecules such as laminin or collagen<sup>18,25,26</sup> are typically immobilized on the hydrogel. PDL is a positively charged, nonspecific ligand, which is expected to facilitate cell adhesion by electrostatic interactions with the cell's membrane.<sup>22,23</sup> Laminin is a well-known ECM protein with specific sites for neuronal attachment and is required for proliferation and migration. Incorporation of PDL or Laminin on PAAm hydrogels has been performed by physisorption<sup>19</sup> or by covalent binding mediated by hydrazinolysis.<sup>12</sup>

Here, we describe a clean and specific method for bifunctional modification of PAAm hydrogels with thiol- and amine-containing biomolecules with controlled densities in an independent, orthogonal manner. By copolymerizing AAm with methylsulfonyl (MS) and acrylic acid (AA) comonomers, we obtain PAAm-AA-MS hydrogels with defined mechanical properties and independently tunable concentrations of two different ligands. The copolymerization did not affect physical properties of PAAm hydrogels such as stiffness, transparency, and biocompatibility. The quantitative and selective covalent binding on hydrogels was explored by UV spectroscopy, using amine- and thiol-containing chromophores as probes. With this strategy, we specifically and covalently immobilized polylysine and a laminin-mimetic peptide, and we analyzed the effect of binding these two components by different protocols on the maturation of cultured postmitotic cortical neurons. We found that neurons cultured for 5 days on hydrogels specifically bifunctionalized exhibited high maturation levels, displaying significantly higher number of neurites, branches, and dendritic

filopodia than cells on hydrogels which were nonspecifically functionalized.

The approach presented here is robust, reproducible, and extensible to the study of the differentiation of other types of progenitor cells, since PAAm hydrogels of diverse mechanical properties can be independently loaded with thiol- and amine-containing ligands of very different molecular weight such as short peptides, ECM proteins, or biopolymers.

## 2. EXPERIMENTAL SECTION

**Materials and Methods.** *2.1. Materials.* Methylsulfonyl comonomer *N*-(4-(5-(methylsulfonyl)-1,3,4-oxadiazol-2-yl)phenyl)-acrylamide (MS) was synthesized as previously reported.<sup>15</sup> The RGD peptides containing chromophores for the quantitative determination of ligand density within the hydrogels were synthesized by using previously reported protocols: cyclo[RGD(DMNPB)fK],<sup>27</sup> cyclo[RGD(DMNPB)fC],<sup>28</sup> cyclo[RGD(coum)fK],<sup>29</sup> and cyclo-[RGD(coum)fC. IK-19 peptide (sequence CSRARKQAASIKVAV-SADR) and poly-D-lysine (PDL) were obtained from Alfa Aesar. Laminin HiLyte was obtained from Cytoskeleton (Denver, U.S.A.), streptavidin-SH and Thiol-PEG-fluorescein 1 kDa from Nanocs Inc. (NY, U.S.A.), and Atto425-biotin from Sigma-Aldrich (Germany). All other chemicals were purchased from Sigma-Aldrich and used as received. UV-vis spectra were recorded with a Varian Cary 4000 UV-vis spectrometer (Varian Inc. Palo Alto, U.S.A.).

*2.2. Preparation of PAAm Hydrogel Films.* PAAm-AA-MS hydrogels were prepared following adapted reported procedures.<sup>6,15,30</sup>

Briefly, acrylamide (18 wt %) was dissolved in phosphate-buffered saline (PBS) (1 mL), acrylic acid (AA) (1.8 wt %), and *N,N*-methylene-bis-acrylamide (0.2 wt %) were added and the pH of solution was adjusted to pH 8 by using 0.1 M NaOH aq solution. Methylsulfonyl comonomer (MS) (0.4 wt %) was dissolved in dimethylformamide (DMF) (125  $\mu$ L) and mixed with the monomer solution. The solution was degassed to remove oxygen, and the free radical initiator ammonium persulfate (10% solution, 1/100 of total volume) and *N,N,N',N'*-tetramethylethylenediamine catalyst (1/1000 of total volume) were added. Ten microliter drops of the polymer solution were placed on Sigmacote-coated glass slides and covered with 3-acryloxypropyl-trimethoxysilane (APM) functionalized coverslips. The hydrogel formed between both glass slides and anchored to APM-coated slides. After 5 min, the hydrogel bound to the APM-coated coverslip was separated from the Sigmacote slide and kept in cold deionized water until further use. Hydrogels prepared this way had a storage modulus ( $G'$ ) of 23 kPa as obtained from dynamic mechanical analysis (DMA) measurement. Control PAAm hydrogels (lacking either AA or MS comonomers) were also prepared by the same method. The hydrogels were dried in a stream of nitrogen before UV measurement. Hydrogels are denoted in the following as PAAm-AA for Poly(acrylamide-co-acrylic acid) and PAAm-AA-MS for Poly(acrylamide-co-acrylic acid-co-methylsulfonyl). The complete characterization of the hydrogels, including measurement of swelling ratio, storage modulus (by DMA), and surface morphology by scanning electron microscopy (SEM) was performed following reported protocols<sup>15</sup> and is fully described in the [Supporting Information](#).

*2.3. Peptide Coupling to PAAm-AA-MS Hydrogels.* Coupling of thiol-peptides to hydrogels was done by incubating the hydrogels with a peptide solution of different concentrations (0.25, 0.5, 0.75, 1.0, 1.5, and 2 mg/mL) in PBS for 1 h at room temperature. Twenty microliters of the peptide solution was placed on a Parafilm surface and covered with the hydrogel. After coupling, the hydrogel was washed with water and with 0.05 M aq acetic acid solution (pH = 3) to rinse out nonspecifically adsorbed peptide, followed by drying under nitrogen stream and measurement of UV absorbance.<sup>15</sup>

Coupling of amine-peptides required prior activation of the -COOH groups of the hydrogel. Incubation of the hydrogel in aqueous solution of 0.2 M *N*-(3-(dimethylamino)propyl)-*N'*-ethylcarbodiimide hydrochloride (EDC), 0.1 M *N*-hydroxysuccinimide (NHS), 0.1 M 2-(*N*-morpho)-ethanesulfonic acid (MES), and 0.5 M

**Table 1.** Chemical Structure of PAAm-AA-MS Constituting Comonomers, Molecular Weight and Polydispersity of Linear (Co)Polymers, and Swelling Ratio and Storage Modulus of Derived Hydrogels

polymer	linear		hydrogel	
	Mn	polydispersity (PD)	swelling ratio [mass water/mass polymer]	storage modulus $G'$ [kPa]
PAAm-AA	79320	2.43	$23.0 \pm 0.2$	$25.6 \pm 1.3$
PAAm-AA-MS	60867	2.56	$21.0 \pm 0.5$	$22.5 \pm 2.3$
PAAm-MS	69852 <sup>a</sup>	2.38 <sup>a</sup>	$6.3 \pm 0.3$	$22.9 \pm 2.1$
PAAm <sup>15</sup>	75194 <sup>a</sup>	2.30 <sup>a</sup>	$5.6 \pm 0.5$	$24.4 \pm 1.1$

<sup>a</sup>Values taken from ref 15.

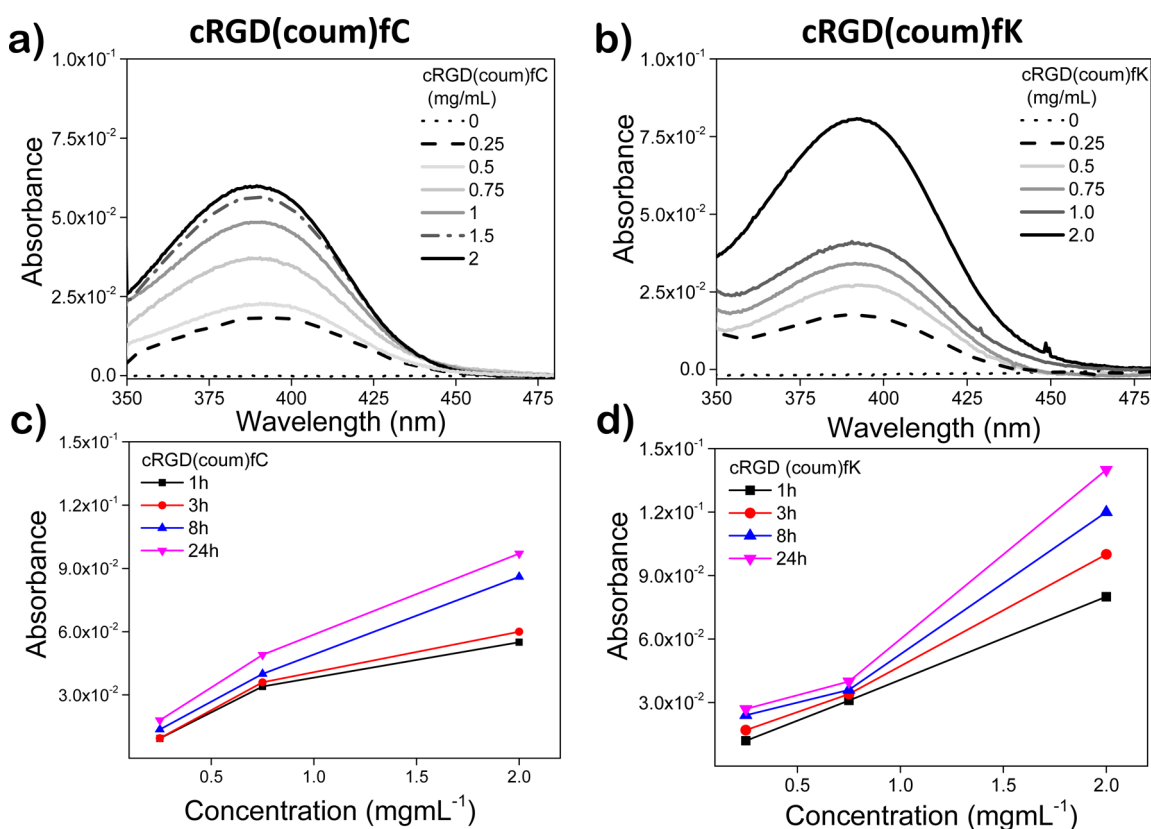


**Figure 1.** UV spectra of PAAm-AA-MS hydrogels after coupling cRGD(coum)fC (left) or cRGD(coum)fK (right) at increasing peptide solution concentrations at room temperature. (a,b) coupling for 1 h, (c,d) coupling at increasing coupling times (1 to 24 h,  $\lambda_{\max} = 390$  nm). Note that there are 9% of  $-\text{COOH}$  groups for amine binding vs 2% of MS groups for thiol binding on the hydrogels.

NaCl for 15 min, was followed by incubation with peptide solutions of different concentrations (0.25–2 mg/mL) in PBS (pH 7.4) for 1 h. The hydrogel was washed with water and 0.05 M acetic acid solution (pH = 3) to rinse out nonspecifically adsorbed peptide, followed by measurement of UV absorbance in dry state.

**Sequential Coupling of Thiol- and Amine-Containing Peptides.** It was carried out by using cRGD(coum)fC and cRGD(DMNPB)fK ( $1 \text{ mg mL}^{-1}$ ) as probes. For testing thiol/amine coupling pathway, hydrogel was functionalized with cRGD(coum)fC followed by washing and measurement of UV absorbance. Subsequently, on the same hydrogel, carboxylic groups were activated by EDC/NHS followed by coupling with cRGD(DMNPB)fK and UV measurement. The amine/thiol route was also tested by first coupling amine peptides using EDC/NHS activation and followed by coupling of thiol peptide.

**Simultaneous Orthogonal Coupling of Thiol- and Amine-Peptides.** To this end, PAAm-AA-MS hydrogel was first activated with EDC/NHS and then incubated with a 1:1 mixture of 1 mg/mL cRGD(coum)fC and cRGD(DMNPB)fK aqueous solution for 1 h, followed by washing and measurement of UV spectra.

**2.4. Determination of Ligand Binding Efficiency to Hydrogels.** The concentration  $C$  of ligand coupled to hydrogels was estimated from the UV absorbance  $A$  using the Lambert–Beer law

$$C = \frac{A}{\epsilon l}$$

where the path length  $l$  = swollen thickness of the hydrogel,  $\epsilon_{\max}$  from coum chromophore ( $20\,000 \text{ M}^{-1} \text{ cm}^{-1}$  at  $\lambda_{\max} 390 \text{ nm}$ ).<sup>29</sup> The binding

efficiency was the ratio between initial concentration of the incubation solution and the final concentration on hydrogel.

**2.5. Functionalization of Hydrogels with PDL and IK-19.** For preparation of substrates modified with PDL alone ( $0.01 \text{ mg mL}^{-1}$ ) and simultaneous IK-19/PDL ( $0.1/0.01 \text{ mg mL}^{-1}$  premixed solution), PAAm-AA-MS hydrogels ( $G' = 23 \text{ kPa}$ ) were first activated by  $0.2 \text{ M}$  EDC,  $0.1 \text{ M}$  NHS,  $0.1 \text{ M}$  2-(*N*-morpho)-ethanesulfonic acid, and  $0.5 \text{ M}$  NaCl for 15 min, followed by coupling with peptide(s) solution. PAAm-AA-MS hydrogels functionalized with IK-19 alone ( $0.01 \text{ mg mL}^{-1}$ ) were modified by incubating the hydrogel for 1 h at room temperature with peptide solution, followed by washing and sterilization with ethanol.

Hydrogels functionalized with PDL and IK-19 by the *sequential* procedure were prepared as follows. PAAm-AA-MS hydrogels were first activated with EDC/NHS as explained above, followed by coupling with PDL solution ( $0.01 \text{ mg mL}^{-1}$ ) and rinsing. Subsequently, the modified hydrogel was incubated with IK-19 solution ( $0.01 \text{ mg mL}^{-1}$ ) for 1 h at room temperature, rinsed, and sterilized with ethanol. All peptide solutions were prepared in PBS.

**2.6. Functionalization of Glass Substrates with IK-19/PDL Mixture ( $0.1/0.01 \text{ mg mL}^{-1}$ ) as Control.** Glass substrates were incubated with 1% 3-aminopropyl-triethoxysilane solution (in 95% ethanol) for 15 min followed by washing with ethanol and baking for 30 min at  $90^\circ\text{C}$ . The glasses were activated with 8% aq glutaraldehyde solution for 6 h, washed with water, and incubated overnight with IK-19/PDL ( $0.1/0.01 \text{ mg mL}^{-1}$ ) solution. Glass substrates were washed with water and sterilized with ethanol.

**2.7. Cell Culture.** Cerebral cortex from E14.5 of C57BL/6 mice was digested in  $0.5\%$  trypsin EDTA (GIBCO) for 15 min at  $37^\circ\text{C}$ . Then trypsin was inactivated by the plating medium (DMEM (GIBCO) and  $10\%$  FBS (Hyclone)) and gently triturated with a 5-ml disposable pipet to get single cells. Centrifugation at  $1000 \text{ rpm}$  was performed for 5 min. Cell pellets were resuspended in  $1 \text{ mL}$  differentiating medium (low glucose DMEM/F12 (GIBCO) and  $2\%$  B27 (Invitrogen)), and cell number was counted. The hydrogel samples having different bound biomolecules were placed in 24-well cell culture plates with  $2.6 \times 10^4/\text{cm}^2$  cells. Cell growth was followed by regular intervals and cells were fixed after 5 days.

**2.8. Immunostaining.** Postmitotic cortical neurons (CNs) were fixed with  $4\%$  Paraformaldehyde (PFA) solution for 10 min, washed three times with PBS pH 7.4, and blocked and permeabilized with  $2\%$  bovine serum albumin (BSA) and  $0.2\%$  Triton in PBS for 45 min at room temperature. The cells were incubated at room temperature with (1:700 DCX (guinea pig, Neuronal lineage marker, dianova) and 1:1000 SMI-312 (Anti Pan-axonal Neurofilament mouse IgG1, Biolegend)) for 2 h. Cells were washed three times with PBS followed by incubation for 2 h at room temperature with (1:800 Cy3 antiguinea pig and 1:1000 alexa-488 antimouse). The nucleus was stained by DAPI and mounted by following standard protocols. Images were taken with Zeiss Axio Observer microscope at  $0.22$  and  $0.42 \mu\text{m}$  per px. Time lapse videos were recorded in order to calculate cell viability and proliferation. The length of axon was measured using Fiji software. The number of branches, processes and spines were quantified manually.

**2.9. Statistical Analysis.** Data were expressed as mean  $\pm$  standard deviation. For each condition, a minimum of three independent experiments were performed. Sample size was bigger than 50 measurements for all experiments. In all cases, a value of  $\alpha < 0.05$  was used for statistical significance. A one-way ANOVA with a Tukey test of the variance was used to determine the statistical significance between groups. In all cases, we have compared the *sequential* coupling condition against all others, and significance difference was set to  $*\alpha < 0.05$ ,  $**\alpha < 0.01$ ,  $***\alpha < 0.001$ .

### 3. RESULTS AND DISCUSSION

PAAm-AA and PAAm-AA-MS hydrogels were prepared by free radical copolymerization of acrylamide (AAm), acrylic acid (AA) and methylsulfonyl acrylate (MS) as comonomers, and bis-acrylamide (bisAAm) as cross-linker. MS and AA were

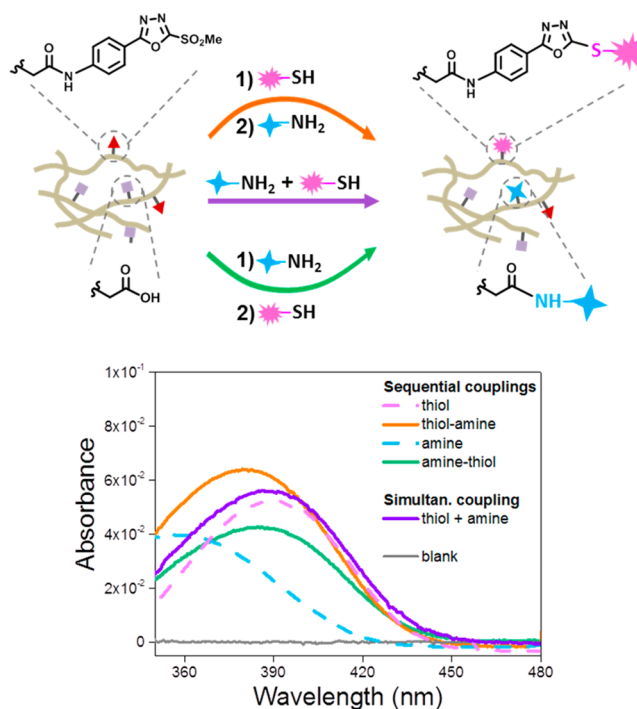


**Figure 2.** Reaction scheme and UV spectra of PAAm-AA-MS hydrogels after sequential incubation first with thiol- and then with amine-containing molecules at  $1 \text{ mg/mL}$  concentration for 1 h at room temperature (orange curve) or in the inverse order (green curve). The simultaneous coupling of the two molecules was also tested (violet curve). The thiol probe was cRGD(coum)fC ( $\lambda_{\text{max}}$  ca.  $390 \text{ nm}$ ), and the amine probe was cRGD(DMNPB)fK ( $\lambda_{\text{max}}$  ca.  $360 \text{ nm}$ ).

**Table 2. Details of the Bifunctionalization of PAAm-AA-MS Hydrogels with PDL and IK-19 Peptide**

substrate	preactivation	bifunctionalization strategy		experiment denoted as
		coupled molecule(s)		
		PDL	IK-19	
PAAm-AA-MS hydrogels	EDC/NHS	yes	no	<i>PDL</i>
	none	no	yes	<i>IK-19</i>
	EDC/NHS	yes	yes	<i>simultaneous</i>
		both molecules at once		
	EDC/NHS	yes (first)	yes (second)	<i>sequential</i>
glass (control)	silanization and glutaraldehyde	yes	yes	<i>mixture glass</i>
		both molecules at once		

incorporated in 2.2 and 8.8 wt % to the monomer mixture, respectively. The amount of MS comonomer used is limited for solubility reasons, whereas an AA percentage close to 10% has proved successful elsewhere.<sup>6</sup> These functional groups allow specific bioconjugation of thiol- and amine-containing biomolecules to the hydrogel.

The introduction of a comonomer in a radical polymerization reaction can influence the polymerization kinetics and the final properties of the PAAm hydrogel. In order to test the effect of the comonomer in PAAm, we first copolymerized PAAm with AA and MS mixtures to form linear copolymers, and we compared their properties with the homopolymer PAAm (Table 1). Linear PAAm-AA copolymers with 8.8% AA showed

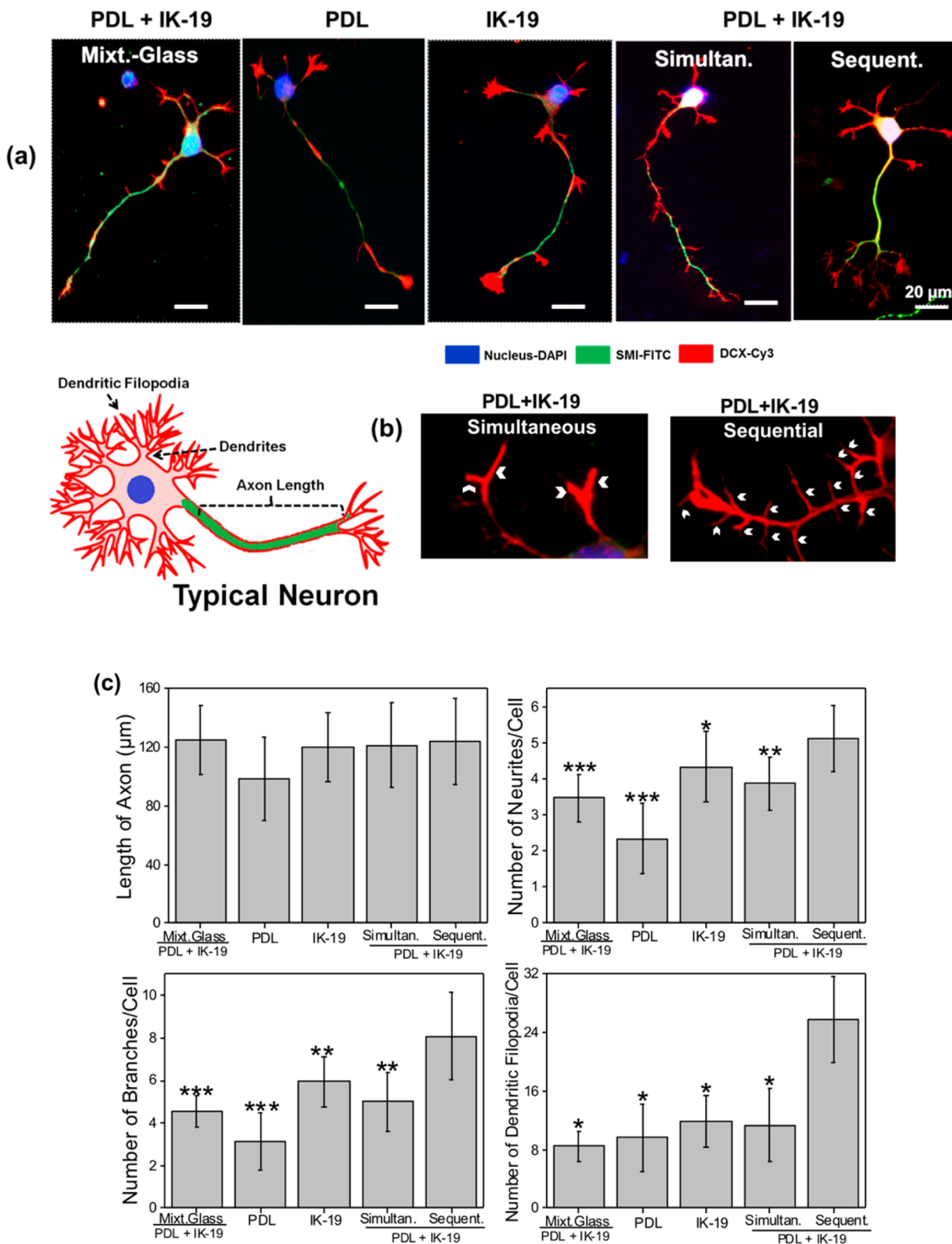


**Figure 3.** Postmitotic cortical neurons (CNs) from mouse embryo (E-14.5) culture after 5 days seeding on PAAm-AA-MS hydrogels. (a) Representative pictures of single neuron developed under different scenarios. (b) High-magnification images depicting distributions of dendritic filopodia on neuronal process. Arrows show the type of counted filopodia. (c) Quantification of axonal length, amount of neurites, branches, and dendritic filopodia developed in newborn neurons after 5 DIV. Significant differences showed in the graphics are compared against sequential substrate.

similar molecular weight and polydispersity to PAAm. PAAm-AA derived hydrogels (with cross-linker) showed higher

swelling and slightly lower storage modulus than PAAm parent hydrogels. SEM studies of freeze-dried samples showed no

significance differences in the morphology of homo- vs copolymer (see [Supporting Information](#)). Similar studies on PAAm-MS copolymers (2.2 wt % MS) showed no noticeable differences in molecular weight, swelling, storage modulus, or morphology to PAAm.<sup>15</sup> When the three comonomers were mixed to prepare PAAm-AA-MS, the resulting copolymer showed swelling properties similar to PAAm-AA. In summary, MS and AA comonomers are incorporated in the AAm chain without affecting the polymerization reaction. The copolymerization of AA leads to higher water uptake in the hydrogel as a consequence of the ionic character of the  $-\text{COOH}$  side group of AA.

We subsequently investigated the specific and selective conjugation of thiol- and amine-containing bioligands to PAAm-AA-MS hydrogels. In order to quantify ligand concentration in the hydrogel, we used ligands containing a chromophore and measured UV spectroscopy on the modified hydrogels. We selected cell-adhesive cyclic RGD peptides containing 7-(*N,N*-diethylamino)-4-(hydroxymethyl)-coumarin (*coum*) group as chromophore. Coum presents a major absorption UV band at around 390 nm.<sup>29</sup> The cyclic peptides c[RGD(*coum*)fC] and c[RGD(*coum*)fK] present either cysteine or lysine as probes for thiol and amine coupling. Coupling of increasing concentrations of c[RGD(*coum*)fC] to PAAm-AA-MS at room temperature for 1 h caused an increase in UV absorbance at  $\lambda \approx 390$  nm, indicating effective and concentration-dependent loading of the thiol-containing ligand on the hydrogel ([Figure 1a](#)). Coupling of c[RGD(*coum*)fK] to PAAm-AA-MS hydrogels at room temperature for 1 h after EDC/NHS activation was also successful ([Figure 1b](#)), though achieved coupling densities were lower than for c[RGD(*coum*)fC] at comparable coupling conditions. Longer incubation times (up to 24 h) lead to an increase in peptide loading in both cases ([Figure 1c,d](#)). This effect was more pronounced in amine coupling. Two scenarios might explain this result: the kinetics of thiol binding is faster than amine at our coupling conditions ([Figure S4](#)), or the binding of amine ligands to NHS-activated carboxylic groups is hindered because of the observed decreased swelling of PAAm-AA-MS gels after NHS activation ([Table S1](#)).<sup>31</sup> Thiol coupling to PAAm-MS hydrogels had an efficiency of >90% after 1 h,<sup>15</sup> whereas thiol coupling to PAAm-AA-MS hydrogels was found to be slower ([Figure 1c](#)) and less efficient. The reason for the negative effect of the AA units in the coupling efficiency of thiols to PAAm-AA-MS hydrogels remains unclear at this point. Note that both ligands were coupled at pH 7.4. Other working pHs might lead to higher coupled ligand densities and will need to be optimized for each target ligand.<sup>32</sup>

To prove the chemoselectivity in the binding reaction, control experiments were performed. PAAm-AA hydrogels (lacking MS) did not show any absorbance after EDC/NHS activation and incubation with thiol-containing ligand. Similarly, no amine coupling was seen on PAAm-AA-MS hydrogels without EDC/NHS activation ([Figure S3](#), [Supporting Information](#)). Overall, these results show that thiol and amine ligands can be specifically bound to our hydrogels in controllable densities.

We analyzed and compared the swelling properties of PAAm-AA-MS hydrogels in PBS after the different coupling steps by gravimetry. EDC/NHS treatment of PAAm-AA-MS hydrogels resulted in a reduced swelling to values comparable to PAAm-MS gels (lacking AA). The esterification of carboxylic groups during EDC/NHS activation step reduced the density of free

ionizable  $-\text{COOH}$  side groups in the hydrogel and lead to lower swelling ratios. NHS activated PAAm-AA-MS gels maintained in PBS for 24 h recovered 35% on the initial swelling before activation, presumably as a consequence of partial hydrolysis of NHS groups and recovery of  $-\text{COOH}$  groups. Control PAAm-AA-MS gels first equilibrated in MES buffer (without EDC/NHS) and then equilibrated in PBS recovered 73% of the initial swelling ([Table S1](#)). This result indicates that the pH change from PBS to MES buffer might cause partial, irreversible collapse of the hydrogel. We also conducted confocal microscopy measurements of the thickness of fluorescently labeled hydrogel films and compared them with the swelling analysis of bulk samples ([Table S2](#) and [Figure S6](#), [Supporting Information](#)). NHS-activated PAAm-AA-MS thin films showed a 3-fold decrease in thickness, from 205 to 63  $\mu\text{m}$ , after NHS activation, in agreement with the measurements on bulk samples. The fluorescence signal was homogeneously distributed along the gel thickness, indicating that bound fluorescent ligands were uniformly distributed across the hydrogel.

We then explored the orthogonal conjugation of thiol and amine biomolecules to the same hydrogel in two sequential incubation steps ([Figure 2](#)). In order to follow individual binding to the two different comonomers, we used RGD peptides containing two different chromophores: cRGD(*coum*)fC ( $\lambda_{\text{max}}$  ca. 390 nm,  $\epsilon_{390} = 20\,000\ \text{M}^{-1}\ \text{cm}^{-1}$ ) and cRGD(DMNPB)fK, ( $\lambda_{\text{max}}$  ca. 360 nm,  $\epsilon_{360} = 4100\ \text{M}^{-1}\ \text{cm}^{-1}$ ). Two different sequential procedures were performed. In one case, thiol was coupled first followed by amine coupling ([Figure 2](#), orange curve). In the second case, the ligands were coupled in the inverse order (green curve on [Figure 2](#)). After incubation and washing, the modified hydrogels showed a clear UV absorption band at  $\lambda_{\text{max}}$  380–385 nm, resulting from the overlap of the two chromophores and demonstrating that both peptides can be effectively linked to the same bifunctional hydrogel. The coupling density depended on the order of the coupling sequence. The first coupling step was ca. twice more efficient than the second. The possibility of simultaneous biofunctionalization was also tested by incubating EDC/NHS activated hydrogels with a 1:1 premixed solution of both peptides ([Figure 2](#), violet curve). In this case, thiol coupling efficiency was similar to the one observed in the thiol–amine sequence, but amine coupling efficiency dropped significantly.

In summary, these results demonstrate that PAAm-AA-MS hydrogels allow effective and selective functionalization with amine- and thiol-containing molecules at tunable concentrations by changing the incubation conditions and protocols. The modified hydrogels retain the low unspecific binding of PAAm hydrogels.

We also tested the bifunctionalization of our gels with larger proteins. We first bound Hilyte-labeled laminin ( $M_w \sim 850$  kDa) by amine coupling. Absorption at  $\lambda_{\text{max}}$  590 nm proved successful coupling (see [Figure S5](#) in the [Supporting Information](#)). Subsequently, we bound streptavidin (75 kDa) through thiol coupling, followed by incubation with biotin-Atto425 (0.71 kDa), which resulted in a noticeable increase in absorption at  $\lambda_{\text{max}}$  425 nm. This result shows that our gels can support functionalization with larger ligands such as ECM components. We have recently reported the binding of rhodamine-labeled fibronectin ( $M_w \sim 440$  kDa) to PAAm-MS gels.<sup>15</sup>

Having demonstrated the ability of our substrates to couple thiol- or amine-presenting molecules orthogonally, we sub-

sequently tested their performance as cell culture platforms presenting two adhesive molecules. As a proof of principle, we decided to study the maturation of postmitotic cortical newborn neurons on PDL and laminin adhesive coatings. PDL is used in neuronal cultures for attachment of neurons through electrostatic interactions. Laminin is an abundant ECM protein in brain tissue; it improves spreading and growth of cultured neurons<sup>33</sup> and promotes extension of neurites.<sup>34</sup> These are desirable features for enhancing neuron maturation. The commercially available IK-19 peptide (sequence CSRARK-QAASIKVAVSADR) is a short mimetic peptide of adhesive site on laminin alpha chain. This peptide stimulates neurite growth, branching, and maturation by interaction with integrin receptors such as  $\alpha_3\beta_1$ ,  $\alpha_4\beta_1$ ,  $\alpha_6\beta_1$ <sup>35</sup> and is frequently used for neuronal cultures as replacement for laminin. In our studies, we used the cysteine-containing IK-19 peptide to be coupled to the MS comonomer of PAAm-AA-MS hydrogels, and we coupled PDL to the EDC/NHS-activated AA comonomer.

We functionalized PAAm-AA-MS hydrogels in different ways (see Table 2): with PDL, with IK-19, with both components sequentially or with a mixture of both components (PDL+IK-19). For comparison, cells were also seeded on standard glass substrates modified by a mixture of PDL+IK-19 (denoted as *mixture glass*) by using glutaraldehyde as bifunctional cross-linker, which reacts with amine on both functionalized glass and on the molecules. For this study, we chose to work with hydrogels of  $G' = 23$  kPa because they are easier to handle and quantify than softer hydrogels ( $\sim 0.2$  kPa) and yet stiff enough<sup>36</sup> to decouple the effect of stiffness over neuronal cell fate and allow for direct comparison with classical glass substrates.

Postmitotic cortical neurons (CNs) from mouse embryo (E-14.5) were seeded on the functionalized hydrogels and cultured for 5 days. No significant differences in cell viability were detected among the different conditions after 24 h of culture. However, cells cultured on our copolymer hydrogels showed a significant improvement of cell survival (23%) after 5 days (Figure S7). We quantified cell maturation by measuring the average number of neurites, the axonal length, the neurite branching and the developed dendritic filopodia after 5 days. All functionalized PAAm-AA-MS hydrogels supported attachment of CNs and promoted the growth of neurites, branches, and dendritic filopodia after 5 days (Figure 3a). No significant differences in the axonal length were found among the different substrates. The presence of IK-19 increased the number of neurites and branches. *Simultaneous* coupling of IK-19 and PDL did not improve neurite formation, branching or formation of dendritic filopodia (see SI). However, bifunctionalization of PAAm-AA-MS hydrogels by *sequential* coupling of PDL and IK-19 using our selective coupling strategy, lead to a significant enhancement of dendritic filopodia formation (3-fold) (Figure 3b,c). Dendritic filopodia are the morphological precursors of neuronal spines,<sup>37</sup> which are required for neuronal synapses and enhance neuronal complexity.<sup>38</sup>

These results show that the coupling strategy for biofunctionalization of PAAm hydrogels has a relevant impact on cell culture. We attribute the improved performance of sequential PDL/IK-19 coupling for neuronal maturation to two reasons: (a) the coupling of short peptide is not hampered by the big PDL molecule, leading to higher IK-19 densities, and (b) the bound IK-19 retains a higher activity due to the chemoselective immobilization through its terminal thiol group. Note that IK-19 peptide contains two lysine rests in the chain,

one of them at the IKVAV epitope, and thus, its nonselective immobilization via those amine side groups during *simultaneous* coupling may be responsible for an impaired activity of the short laminin peptide. This highlights the value of our orthogonal coupling regarding bioactivity retention of chemoselectively bound ligands.

It is generally accepted that neuronal growth and differentiation is favored on soft substrates with elasticity modulus in sub-kPa range.<sup>20</sup> We therefore extended our study to 0.17 kPa hydrogels bifunctionalized with PDL+IK-19 components (Figure S8). As expected, softer substrates supported neuron growth and differentiation, showing slightly increased axon length ( $\sim 13\%$ ) and number of neurites ( $\sim 17\%$ ) compared to stiffer hydrogels. We found significantly longer axons and higher number of neurites for cells cultured on *sequential* substrates in comparison to *simultaneous* coupling but no significant differences in number of branches. These results show that our strategy is robust and easily extensible to PAAm hydrogels with diverse mechanical properties.

#### 4. CONCLUSIONS

We have demonstrated that bifunctional PAAm-AA-MS hydrogels can couple molecules containing amine and thiol groups with high chemical selectivity, efficiency, and functionality. These properties allowed enhanced maturation of neuronal cultures on PAAm hydrogels. This hydrogel platform can be expanded to other adherent molecules. Our approach is robust, reproducible, and extensible to the study of adhesive factors for the differentiation of other types of progenitor cells. PAAm-AA-MS hydrogels of diverse mechanical properties can be independently loaded with thiol- and amine-containing ligands of very different molecular weight such as short peptides, ECM proteins, or biopolymers.

#### ■ ASSOCIATED CONTENT

##### 📄 Supporting Information

The Supporting Information is available free of charge on the ACS Publications website at DOI: 10.1021/acs.biomac.6b01784.

Detailed physicochemical characterization of hydrogels and supporting UV spectroscopy, swelling ratio, confocal microscopy, and cell culture results (PDF)

#### ■ AUTHOR INFORMATION

##### Corresponding Authors

\*E-mail: [julieta.paez@leibniz-inm.de](mailto:julieta.paez@leibniz-inm.de). Tel: +49(0)681-9300-369.

\*E-mail: [aranzazu.delcampo@leibniz-inm.de](mailto:aranzazu.delcampo@leibniz-inm.de). Tel: +49(0)681-9300-510. Fax: +49(0)681-9300-223.

##### ORCID

Julieta I. Paez: 0000-0001-9510-7254

##### Author Contributions

The manuscript was written through contributions of all authors. All authors have given approval to the final version of the manuscript.

##### Notes

The authors declare no competing financial interest.

#### ■ ACKNOWLEDGMENTS

A.F. thanks the financial support from the Max-Planck Graduate Center during her Ph.D. program.

## REFERENCES

- (1) Kyburz, K. A.; Anseth, K. S. *Ann. Biomed. Eng.* **2015**, *43* (3), 489–500.
- (2) Lv, H.; Li, L.; Zhang, Y.; Chen, Z.; Sun, M.; Xu, T.; Tian, L.; Lu, M.; Ren, M.; Liu, Y.; Li, Y. *Cell Tissue Res.* **2015**, *361* (3), 657–668.
- (3) Banks, J. M.; Mozden, L. C.; Harley, B. A. C.; Bailey, R. C. *Biomaterials* **2014**, *35* (32), 8951–8959.
- (4) Caliari, S. R.; Burdick, J. A. *Nat. Methods* **2016**, *13* (5), 405–414.
- (5) Denisin, A. K.; Pruitt, B. L. *ACS Appl. Mater. Interfaces* **2016**, *8*, 21893–21902.
- (6) Zouani, O. F.; Kalisky, J.; Ibarboure, E.; Durrieu, M.-C. *Biomaterials* **2013**, *34* (9), 2157–2166.
- (7) Li, C.; Allen, J.; Alliston, T.; Pruitt, L. A. *J. Mech. Behav. Biomed. Mater.* **2011**, *4* (7), 1540–1547.
- (8) Trappmann, B.; Gautrot, J. E.; Connelly, J. T.; Strange, D. G. T.; Li, Y.; Oyen, M. L.; Cohen Stuart, M. A.; Boehm, H.; Li, B.; Vogel, V.; Spatz, J. P.; Watt, F. M.; Huck, W. T. S. *Nat. Mater.* **2012**, *11* (7), 642–649.
- (9) Rape, A. D.; Guo, W. H.; Wang, Y. L. *Biomaterials* **2011**, *32* (8), 2043–2051.
- (10) Théry, M. *J. Cell Sci.* **2010**, *123* (24), 4201–4213.
- (11) Pande, C.; Sharma, A. *J. Appl. Polym. Sci.* **2002**, *84* (14), 2613–2620.
- (12) Damljanović, V.; Lagerholm, B. C.; Jacobson, K. *BioTechniques* **2005**, *39* (6), 847–851.
- (13) Grevesse, T.; Versaavel, M.; Circelli, G.; Desprez, S.; Gabriele, S. *Lab Chip* **2013**, *13* (5), 777–780.
- (14) Seiffert, S.; Oppermann, W. *Macromol. Chem. Phys.* **2007**, *208* (16), 1744–1752.
- (15) Farrukh, A.; Paez, J. I.; Salierno, M.; del Campo, A. *Angew. Chem., Int. Ed.* **2016**, *55* (6), 2092–2096.
- (16) Huebsch, N.; Arany, P. R.; Mao, A. S.; Shvartsman, D.; Ali, O. A.; Bencherif, S. A.; Rivera-Feliciano, J.; Mooney, D. J. *Nat. Mater.* **2010**, *9* (6), 518–526.
- (17) Wen, J. H.; Vincent, L. G.; Fuhrmann, A.; Choi, Y. S.; Hribar, K. C.; Taylor-Weiner, H.; Chen, S.; Engler, A. J. *Nat. Mater.* **2014**, *13* (10), 979–987.
- (18) Georges, P. C.; Miller, W. J.; Meaney, D. F.; Sawyer, E. S.; Janmey, P. A. *Biophys. J.* **2006**, *90* (8), 3012–3018.
- (19) Franze, K.; Gerdemann, J.; Weick, M.; Betz, T.; Pawlizak, S.; Lakadamyali, M.; Bayer, J.; Rillich, K.; Gögler, M.; Lu, Y. B.; Reichenbach, A.; Janmey, P.; Käs, J. *Biophys. J.* **2009**, *97* (7), 1883–1890.
- (20) Lu, Y. B.; Franze, K.; Seifert, G.; Steinhäuser, C.; Kirchhoff, F.; Wolburg, H.; Guck, J.; Janmey, P.; Wei, E. Q.; Käs, J.; Reichenbach, A. *Proc. Natl. Acad. Sci. U. S. A.* **2006**, *103* (47), 17759–17764.
- (21) Stukel, J. M.; Willits, R. K. *Tissue Eng., Part B* **2016**, *22* (3), 173–182.
- (22) Moshayedi, P.; Costa Lda, F.; Christ, A.; Lacour, S. P.; Fawcett, J.; Guck, J.; Franze, K. *J. Phys.: Condens. Matter* **2010**, *22* (19), 194114.
- (23) Lantoine, J.; Grevesse, T.; Villers, A.; Delhay, G.; Mestdagh, C.; Versaavel, M.; Mohammed, D.; Bruyère, C.; Alaimo, L.; Lacour, S. P.; Ris, L.; Gabriele, S. *Biomaterials* **2016**, *89*, 14–24.
- (24) Kim, Y. H.; Baek, N. S.; Han, Y. H.; Chung, M.-A.; Jung, S.-D. *J. Neurosci. Methods* **2011**, *202* (1), 38–44.
- (25) Barros, C. S.; Franco, S. J.; Müller, U. *Cold Spring Harbor Perspect. Biol.* **2011**, *3* (1), a005108.
- (26) Sun, Y.; Huang, Z.; Liu, W.; Yang, K.; Sun, K.; Xing, S.; Wang, D.; Zhang, W.; Jiang, X. *Biointerphases* **2012**, *7* (1), 29.
- (27) Petersen, S.; Alonso, J. M.; Specht, A.; Duodu, P.; Goeldner, M.; del Campo, A. *Angew. Chem., Int. Ed.* **2008**, *47* (17), 3192–5.
- (28) Lee, T. T.; García, J. R.; Paez, J. I.; Singh, A.; Phelps, E. A.; Weis, S.; Shafiq, Z.; Shekaran, A.; del Campo, A.; García, A. J. *Nat. Mater.* **2015**, *14* (3), 352–360.
- (29) Weis, S.; Shafiq, Z.; Gropeanu, R. A.; del Campo, A. *J. Photochem. Photobiol., A* **2012**, *241*, 52–57.
- (30) Moshayedi, P.; da F Costa, L.; Christ, A.; Lacour, S. P.; Fawcett, J.; Guck, J.; Franze, K. *J. Phys.: Condens. Matter* **2010**, *22* (19), 194114.
- (31) Toda, N.; Asano, S.; Barbas, C. F. *Angew. Chem., Int. Ed.* **2013**, *52* (48), 12592–12596.
- (32) Lahiri, J.; Isaacs, L.; Tien, J.; Whitesides, G. M. *Anal. Chem.* **1999**, *71* (4), 777–790.
- (33) Liesi, P. *EMBO J.* **1985**, *4* (5), 1163.
- (34) Manthorpe, M.; Engvall, E.; Ruoslahti, E.; Longo, F. M.; Davis, G. E.; Varon, S. *J. Cell Biol.* **1983**, *97* (6), 1882–1890.
- (35) Frith, J. E.; Mills, R. J.; Hudson, J. E.; Cooper-White, J. J. *Stem Cells Dev.* **2012**, *21* (13), 2442–2456.
- (36) Engler, A. J.; Sen, S.; Sweeney, H. L.; Discher, D. E. *Cell* **2006**, *126* (4), 677–689.
- (37) Dansie, L. E.; Ethell, I. M. *Dev. Neurobiol.* **2011**, *71* (11), 956–981.
- (38) Yuste, R.; Bonhoeffer, T. *Nat. Rev. Neurosci.* **2004**, *5* (1), 24–34.